Saudi Journal of Biological Sciences 29 (2022) 1–10

Contents lists available at ScienceDirect

Saudi Journal of Biological Sciences

journal homepage: www.sciencedirect.com

Original article

Itraconazole loaded nano-structured lipid carrier for topical ocular delivery: Optimization and evaluation

Manish Kumar [a,*], Abhishek Tiwari [e], Syed Mohammed Basheeruddin Asdaq [c], Anroop B. Nair [d], Shailendra Bhatt [b], Pottathil Shinu [f], Abdulaziz K. Al Mouslem [d], Shery Jacob [g], Abdulhakeem S. Alamri [h,i], Walaa F. Alsanie [h,i], Majid Alhomrani [h,i], Varsha Tiwari [e], Sheetal Devi [a], Ajay Pathania [a], Nagaraja Sreeharsha [d,j]

[a] M.M. College of Pharmacy, Maharishi Markandeshwar (Deemed to be University), Mullana-Ambala, Haryana 133207, India
[b] Department of Pharmacy, School of Medical and Allied Sciences, G.D. Goenka University, Gurugram, Haryana 122103, India
[c] Department of Pharmacy Practice, College of Pharmacy, AlMaarefa University, Dariyah, 13713, Riyadh, Saudi Arabia
[d] Department of Pharmaceutical Sciences, College of Clinical Pharmacy, King Faisal University, Al-Ahsa 31982, Saudi Arabia
[e] Department of Pharmacy, Devsthali Vidyapeeth College of Pharmacy, Lalpur, Rudrapur (Udham Singh Nagar), Uttrakhand 263148 India
[f] Department of Biomedical Sciences, College of Clinical Pharmacy, King Faisal University, Al-Ahsa 31982, Saudi Arabia
[g] Department of Pharmaceutical Sciences, College of Pharmacy, Gulf Medical University, Ajman 4184, United Arab Emirates
[h] Department of Clinical Laboratory Sciences, The Faculty of Applied Medical Sciences, Taif University, Taif, Saudi Arabi
[i] Centre of Biomedical Sciences Research (CBSR), Deanship of Scientific Research, Taif University, Saudi Arabia
[j] Department of Pharmaceutics, Vidya Siri College of Pharmacy, Off Sarjapura Road, Bangalore, 560035, India

ARTICLE INFO

Article history:
Received 5 October 2021
Revised 23 October 2021
Accepted 4 November 2021
Available online 12 November 2021

Keywords:
Itraconazole
Nano-lipid carriers
Ocular
Release
Antifungal activity

ABSTRACT

Background & Objectives: Low penetration efficiency and retention time are the main therapeutic concerns that make it difficult for most of the drugs to be delivered to the intraocular tissues. These challenging issues are often related to those drugs, which have low or poor solubility and low permeability. The goal of this study was designed to develop nanostructured lipid carriers (NLCs) loaded with itraconazole (ITZ) with the objective of enhancing topical ocular permeation and thereby improving clinical efficacy.
Materials and Methods: ITZ-loaded NLCs were fabricated by a high-speed homogenization technique using surfactant (Poloxamer 407), and lipids (stearic acid and oleic acid). Optimization of formulations was performed by 3 level factorial design and the selected formulation (F6) was evaluated by differential scanning calorimetry and transmission electron microscopy. Antifungal activity was assessed by measuring the zone of inhibition and irritation potential using the HET-CAM test.
Results: The independent variables (lipid ratio-X_1 and percentage of emulsifier-X_2) have a positive impact on percentage entrapment efficiency (Y_2) and percentage release (Y_3) but have a negative impact on particle size (Y_1). Based on the better entrapment efficiency (94.65%), optimum particle size (150.67 nm), and percentage cumulative drug release (68.67%), batch F6 was selected for further evaluation. Electron microscopic images revealed that the prepared particles are spherical and have nano size. Antifungal studies demonstrated enhancement in the zone of inhibition by formulation F6 as compared to a commercial eye drop. The non-irritancy of optimized formulation (F6) was confirmed with a zero score.
Interpretation & Conclusion: In summary, the optimized NLCs seem to be a potent carrier for the effective delivery of itraconazole in ocular therapy.

* Corresponding author.
E-mail addresses: manish_singh17@rediffmail.com (M. Kumar), anair@kfu.edu.sa (A.B. Nair), spottathail@kfu.edu.sa (P. Shinu), aalmoslem@kfu.edu.sa (A.K. Al Mouslem), a.alamri@tu.edu.sa (A.S. Alamri), w.alsanie@tu.edu.sa (W.F. Alsanie), m.alhomrani@tu.edu.sa (M. Alhomrani), sharsha@kfu.edu.sa (N. Sreeharsha).
Peer review under responsibility of King Saud University.

Production and hosting by Elsevier

https://doi.org/10.1016/j.sjbs.2021.11.006
1319-562X/

1. Introduction

Designing ocular drug delivery is a difficult task due to the eye's unique anatomy, physiology, and biochemistry. Anatomically eye possesses two sections: anterior and posterior. The posterior segment of the eye roughly involves 33% and the remaining part comprises the back fragment. The anterior segment involves the cornea, iris, conjunctiva, ciliary body, watery diversion, and focal point (Achouri et al., 2013). The sclera, optic nerve, choroid plexus, retina, vitreous silliness is located in the posterior portions and back of the eye. Both anterior and posterior portions of the eye are susceptible to different vision undermining illnesses. The anterior portion is critically susceptible to the waterfall, conjunctivitis, and front uveitis.

The most prevalent disorders that affect the back of the eye are age-related macular degeneration and diabetic retinopathy. Further, it is hard to complete therapy fixation using topical eye drops installation in the back portion of the visual tissues as <5% of the visual tissues are topically connected (Achouri et al., 2013; Balguri et al., 2016; Pandey et al., 2021; Shah et al., 2019b). Fungi, which include *Aspergillus flavus*, *Aspergillus fumigates, Aspergillus niger, Candida species*, *Fusarium*, mainly cause mycotic corneal ulcers. Keratitis, a type of corneal inflammation mainly caused by a fungal etiology and contributes to the majority of the ophthalmic mycosis. Immunocompromised patients are more prone to develop infectious ulcers, particularly after keratoplasty (Hoffman et al., 2021; Jaiswal et al., 2015; Knutsson et al., 2021; Song et al., 2021). Itraconazole (ITZ), an antifungal agent that is used to treat fungal keratitis. Typically, ITZ is a triazole effective against *Curvularia*, *Candida*, and *Aspergillus* species. Few studies have been attempted to deliver ITZ through the cornea by formulating different nanocarriers (ElMeshad and Mohsen, 2016; Permana et al., 2021; Thomas, 2003).

Lipid-based drug delivery systems have the potential capacity to entrap both hydrophobic and hydrophilic molecules, enhance the bioavailability of poorly aqueous soluble drugs, and protect them from untimely degradation. NLC has been reported to be an alternate bioactive delivery system to solid lipid nanoparticles (SLN) in terms of minimum toxicity, biocompatibility, biodegradation, slow drug release, and avoidance of organic solvent during processing (Liu and Wu, 2010). NLC was designed to overcome the disadvantages associated with SLN like crystallinity of solid lipids, which affects the entrapment efficiency and release of the encapsulated drugs (Kamboj et al., 2010). NLCs are made up of biocompatible strong lipid networks and fluid lipids that have distinctly different structures than those derived from solid lipids. In addition, NLCs have the typical molecule distance of 10–1000 nm in the lattice. NLCs are the second-generation SLNs that possess a solid-lipid lattice, which is adjoined by liquid lipids (ElMeshad and Mohsen, 2016). In NLCs, oil droplets are embedded in a solid lipid matrix.Further, liquid lipids are preferable solubilizers of medications over strong lipids. This carrier molecule is made up of biodegradable lipids with low cytotoxicity. NLCs possess several advantages against conventional carriers for drug therapy, which include increased solubility, enhanced stability, enriched permeability, and bioavailability, targeted tissue delivery minimized side effects, sustained half-life (Duong et al., 2020; Fang et al., 2013; Nair et al., 2021a). The small shape of the lipid nanoparticles helps the drug to adhere to the surface of the cornea that further enhancing the concentration of active substances permeating the membrane. The robust lipid lattice of NLCs can impart a strong controlled release of drug molecules entrapped inside this carrier. The nanoscale dimension of NLC enhances pre-corneal residence time and the rate of corneal absorption of ocular drugs via ocular tissues. NLC has pulled in extending logical and commercial thought during the most recent years. This incorporates a high amount of drug preload, enlarge drug strength, the likelihood to control release and focusing on, and shirking of natural solvents (Dhiman et al., 2021; Haider et al., 2020; Hallan et al., 2021; Wissing and Müller, 2001). NLCs are exceptionally effective structures mainly because of their strong lipid networks and their potential to improve the efficacy of various drug molecules *in vitro* as well as *in vivo* (Dhiman et al., 2021). In the context of this, the goal of this study was to fabricate and analyze the possibility for topical ocular delivery of ITZ-loaded NLCs. The potential of NLC formulation to enhance the ocular permeation in rabbit cornea was demonstrated using propranolol hydrochloride, a hydrophilic molecule (Sharif Makhmal Zadeh et al., 2018).

The exponential rise of nanotechnology over the last decades has resulted in the creation of several adaptable drug carriers with a diameter of 10–1000 nm, such as liposomes, polymeric micelles, and SLNs. Encapsulation in nanoparticles with a high specific surface area enhances the stability and solubility of the medication while retaining a minimal adverse effect profile. Drugs that are insoluble in the water though have a high therapeutic potential have benefited the most from nanoencapsulation, which has been proposed as a viable method for bypassing the different ocular barriers. Indeed, considerable research has proven an increase in the bioavailability and residence duration of drugs in ocular target tissues (Morrison and Khutoryanskiy, 2014).

2. Materials and methods

2.1. Chemicals

ITZ and Pluronic F127 (Poloxamer 407) were obtained from Vital Laboratories, Vapi, India, and BASF Corporation, New Jersey, USA, respectively. Stearic acid, oleic acid, calcium chloride, and various inorganic acids were procured from RFCL Ltd. (New Delhi, India). Sodium hydroxide and potassium dihydrogen orthophosphate, and sodium chloride was procured from S.D. Fine Chemicals, Mumbai, India. Linseed oil was obtained from National oil and chemicals, New Delhi, India. All other reagents used were of analytical grade and were used as obtained.

2.2. Formulation of ITZ loaded NLCs

To fabricate ITZ-loaded NLCs, a high-speed homogenization approach was employed by following a method described in the literature (Duong et al., 2020) with minor modifications. The schematic representation of the procedure for the preparation of ITZ-loaded NLCs is displayed in Fig. 1. In brief, the lipid phase consisting of stearic acid and oleic acid (1:1) was obtained by heating both at 85 °C. At the same time, the aqueous phase contains a surfactant (1.6% of poloxamer 407) with ITZ was prepared separately and heated to a similar temperature. Then the lipid phase was added to the aqueous phase and homogenized to obtain emulsion and then further cooled to room temperature to obtain ITZ loaded NLCs. The formulation optimization was carried out by 3^2 factorial design (Jacob et al., 2017) by selecting two independent variables [(lipid ratio (X_1) and percentage of emulsifier (X_2)] and evaluating their impact on three dependent variables [particle size (Y_1), percentage entrapment efficiency (Y_2) and percentage release (Y_3) as depicted in Table 1. To test various responses, nine batches (F1-F9) with low (-1), medium (0), and high (+1) lipid and emulsifier levels were used. The data was statistically authenticated using analysis of variance (ANOVA) (Lim et al., 2014).

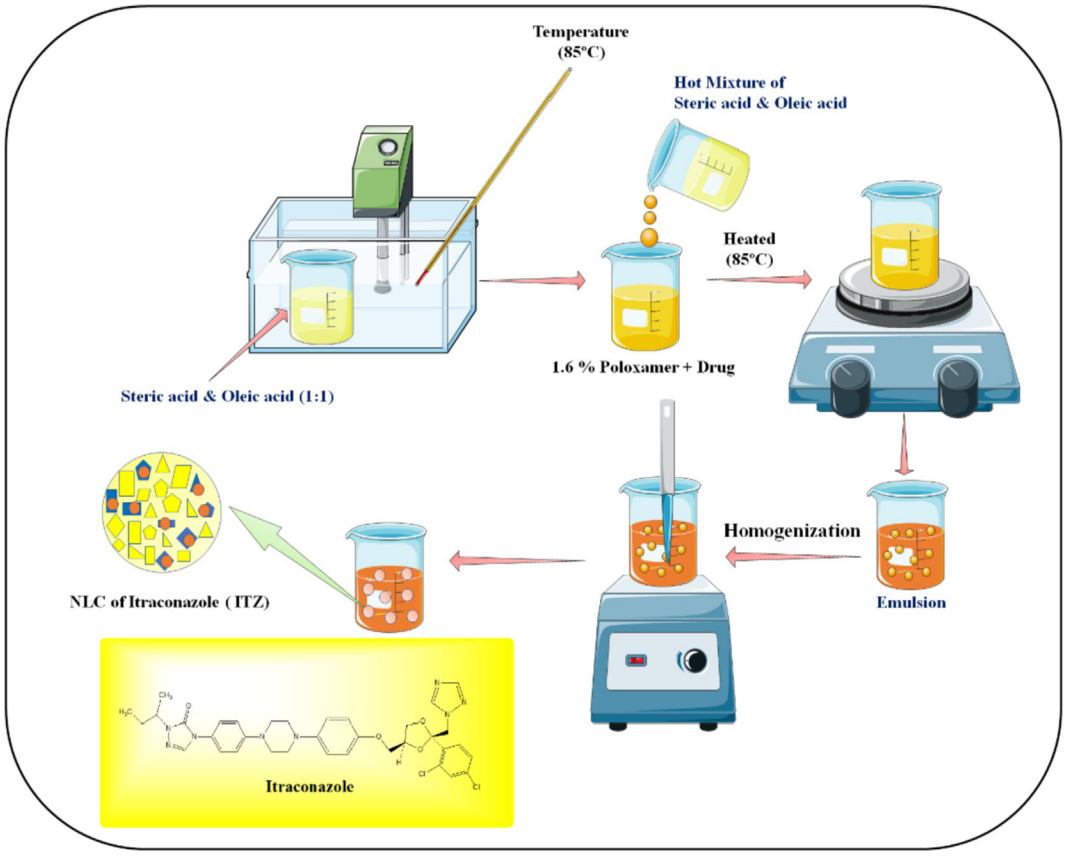

Fig. 1. Schematic representation of the preparation of itraconazole-loaded NLCs by homogenization method.

Table 1
3^2 Factorial design for the itraconazole-loaded nanostructured lipid carriers.

Formulation code	Lipid ratio (X_1)	Emulsifier (X_2) (%)	Response
F1	1:1 (-1)	1 (-1)	
F2	1:1 (-1)	3 (1)	Y_1 = Particle size (nm)
F3	3:1 (1)	3 (1)	
F4	1:1 (-1)	2 (0)	Y_2 = Percentage entrapment
F5	3:1 (1)	1 (-1)	efficiency (% w/v)
F6	2:1 (0)	2 (0)	
F7	2:1 (0)	1 (-1)	Y_3 = Percentage release (%)
F8	3:1 (1)	2 (0)	
F9	2:1 (0)	3 (-1)	
F10*	1.5:0.5	1.5	

2.3. Validation of the experimental design and selection of the best formulation

In our study, the formulation which is having the least particle size, maximum entrapment efficiency, and maximum percent of *in vitro* release for 8 h was selected as the final formulation depending on the response characteristics. The design of each formulation was validated by using software Design expert 13.0.0 (State – Ease, Inc., USA). The response was assessed by the statistical tool with interactive and polynomial terms used:

$$Y = \beta_0 + \beta_1 X_1 + \beta_2 X_2 + \beta_3 X_1 X_2 + \beta_4 X_1^2 + \beta_5 X_2^2 + \beta_6 X_1 X_2^2 + \beta_7 X_1^2 X_2 + \beta_8 X_1^2 X_2^2 r^2$$

In Equation 1, a total of eight coefficients (β_1 to β_8) were calculated with β_0 representing the intercept, and β_4 to β_8 representing the various quadratic and interaction terms, X_1 and X_2 are the coded levels of the independent variables, and X_1 X_2 is the interaction terms, and X_1^2 and X_2^2 are the polynomial terms. The arithmetic mean of all quantities outcomes is 0 from all the nine runs, β1 to β8 are the coefficients computed from the observed experimental values of Y, and 1 to 8 are the coefficients computed from the observed experimental values of Y. To validate the checkpoint formulation (F10) a rigorous grid search was conducted over the experimental domain. From the polynomial equation, the formulation was developed and the actual response was experimentally checked and correlated to the results.

2.4. Particle size

The size of particles in the prepared NLCs was determined by laser diffraction technique using a Malvern Zetasizer (S90 series, Worcestershire, UK) (Morsy et al., 2019). The size of the particles was checked at 25 °C after diluting the drug concentration with deionized purified water and filtered using a syringe filter (pore size 0.45 μm, Millipore Co., USA) (Sreeharsha et al., 2020). For each formulation, the particle size was measured six times and the results are represented as means ± SD.

2.5. Entrapment efficiency (EE)

The amount of ITZ entrapped in the particles was determined after uniformly dispersing the NLCs in water by gentle shaking. Then, methanol (5 mL) was mixed with this dispersion (1 mL) followed by refrigerated centrifugation at 15,000 rpm for 45 min (3 K30, Sigma, Osterode, Germany) (Nair et al., 2019). This dispersion was filtered with a Millipore membrane filter of pore size

0.2 μm (Bedford, MA, USA), and ITZ content was analyzed using a UV spectrophotometer (UV-1280, Shimadzu, Kyoto, Japan) at 262 nm λ max. The % EE was calculated using the below formula;

$$\% \text{ EE} = [\text{W (Total)} - \text{W (Free)}/\text{ W (Total)}] \times 100$$

where W (Total) is the amount of drug added to the NLC and W (Free) is the amount of un-entrapped drug. The % EE was measured six times and the results are represented as means ± SD.

2.6. Release of ITZ from NLCs

The *in vitro* drug release of NLCs (F1-F10) was studied by using a dialysis bag method described elsewhere (Nair et al., 2017). The directions of the manufacturer for the activation of the dialysis membrane (12 kDa cut off) were followed. The experiments were carried out in a sink environment. ITZ-NLCs formulations (10 mg/mL ITZ) were loaded into a cellulose membrane dialysis bag and magnetically stirred at 37 ± 0.5 °C in 200 mL of simulated tear fluid (STF, pH 7.4) (Shah et al., 2019b). The STF solution was prepared by dissolving sodium chloride (0.68 g), sodium bicarbonate (0.22 g), calcium chloride (0.008 g), and potassium chloride (0.14 g) in 100 mL of distilled deionized water. Samples (5 mL) from the receiver solution were taken at predetermined intervals and replaced with the equivalent amount of STF solution at the same temperature. The drug concentration was quantified spectrophotometrically at λmax (262 nm). The release experiment of each formulation was carried out six times and the results are represented as means ± SD.

2.7. Differential scanning calorimetry (DSC)

A DSC instrument (Q200, TA Instruments Trios V4.1, Newcastle, PA, USA) was used to record the thermograms of ITZ, poloxamer, blank NLCs, and ITZ-NLCs (F6). The samples (5 mg) were sealed in an aluminum pan and heated at a rate of 10 °C/min (heating range 10–250 °C). Analysis was carried out under a nitrogen purge at a rate of 50 mL/min. Two standard pans were used, one with 5 mg of sample for analysis and the other with an empty pan as a control (Chaudhary et al., 2021).

2.8. Transmission electron microscopy (TEM)

The morphology of an optimized NLC formulation (F6) was examined using TEM. A single drop of NLCs was placed on a carbon-coated copper disc (400-network), and the excess liquid was removed with the help of tissue paper. A drop of neutralized phosphotungstic acid solution (2% w/v) was added to the framework. The stained samples were air-dried at room temperature before examining at 4000 X. TEM images were taken with an accelerating voltage of 200 kV (Shah et al., 2020).

2.9. Zeta potential

A laser doppler electrophoresis system was employed to quantify particle electrostatic charge using a Malvern Zetasizer (S90 series, Worcestershire, UK) and the observed values were presented as zeta potential (Akrawi et al., 2020). All experiments were carried out in triplicate at physiological pH (7.26 ± 0.13) to simulate physiological conditions.

2.10. In vitro antifungal activity

The antifungal activity was tested using the agar cup-plate method. The activity was calculated by measuring the mean diameter of the zone of inhibition against *Aspergillus niger* and *Aspergillus flavus*. Sabouraud dextrose agar plates were made by autoclaving at 121 °C, and 15 lbs pressure for 15 min. The required amount of melted agar media (300 mL) was combined with *Aspergillus niger* and *Aspergillus flavus* suspension (2 mL of inoculum to 100 mL of molten agar media) and placed into two sterile Petri plates after cooling (42 ± 0.5 °C) the agar. In each Petri plate, three 5 mm wells were drilled with a sterile borer. Then, 0.2 mL of each test substance (ITZ loaded NLC, F6), blank NLC, and standard commercial product (ITZ eye drop; ITRAL, Jawa Pharmaceuticals, Gurugram, India) were transferred aseptically to containers and labeled accordingly. A negative and positive control, which included uninoculated media and media seeded with test organism but deprived of antifungal operability, were also made to ensure the observations of test and standard. The Petri plates loaded with samples were kept at 25 °C for two hours to allow diffusion of the formulation into the medium, and then incubated for 48 h at 28 °C. The diameter of each well's zone of inhibition was measured and the data presented are mean of six trials ± SD (Shah et al., 2019b).

2.11. Irritation potential (HET-CAM Test)

The HET-CAM test was used to determine the ocular irritation studies of the ITZ-loaded NLCs. The test was performed in newly collected fertile eggs, which were incubated at 37 °C ± 0.5 °C and 55% RH in three days. After the hatching time of three days, the eggs were candled to check the suitability of the eggs, and those observed to be nonviable were not included in the examination. The suitable eggs were gathered and again incubated for another ten days. The eggs were manually moved to ensure the adequate growth of CAM. On day 10, the eggshell was removed by applying an external force with a pencil. The hidden film was soaked at 37 °C cautiously with 0.9% sodium chloride solution. The dampening solution was prudently expelled to guarantee that there was no harm to the basic veins. After then, 0.3 mL of positive and negative controls, as well as 0.3 mL of NLCs, were added to the uncovered HET-CAM test. The positive and negative controls used in the experiment were 0.1 M sodium hydroxide and 0.9 percent sodium chloride, respectively. The HET-CAM test was used to look for changes in the surface, including alterations in the vascular structure as a result of aggravation, such as discharge, lysis, and coagulation. The HET-CAM test was scored using the inference described in the literature (Irimia et al., 2018) and the CAM scoring outlined for the HET-CAM test.

3. Results

3.1. Factorial design and mathematical modeling

The 3^2 full factorial designs were used to analyze formulation data produced in the study (design expert software version 9.0.5, State-Ease, Inc., Minneapolis, USA). The evaluation response was analyzed using a statistical model that incorporated both interactive and polynomial terms.

$$Y = b_0 + b_1X_1 + b_2X_2 + b_{12}X_1X_2 + b_{11}X_1^2 + b_{22}X_2^2$$

where Y is the free factor. Where b0, the block is the number juggling means of the fundamental impacts (regression coefficients) b1, b2, b3, b12, b13, b23, and b123 were determined by utilizing the signs in the sections, by adding or deducting the worth of the got reactions, Y. At last, the qualities are summarized with several details. Where X_1 and X_2 are the coded levels of the independent variables and X_1X_2 are the association and polynomial terms, separately. Given the data gained from the smoothed-out subtleties, an overall verifiable model can be portrayed from the above data. The model made can be portrayed by using the polynomial

Table 2
Characterization of itraconazole-loaded NLCs (F1-F10).

Formulation code	Particle size (NM) (Y_1)	Entrapment efficiency (%) (Y_2)	Percentage release (%) (Y_3)
F1	164.14	95.34 ± 1.23	34.8 ± 0.13
F2	152.21	91.43 ± 1.87	42.18 ± 0.40
F3	160.62	60.67 ± 0.67	52.45 ± 1.20
F4	157.87	93.78 ± 1.12	61.56 ± 1.09
F5	166.67	62.17 ± 0.79	51.45 ± 0.93
F6	150.67	94.65 ± 0.98	68.67 ± 0.53
F7	153.40	93.06 ± 0.68	48.89 ± 0.23
F8	165.96	91.54 ± 0.16	58.44 ± 0.76
F9	175.39	90.76 ± 1.71	61.23 ± 0.73
F10*	179.12	93.61 ± 0.89	46.19 ± 0.67

F10*= extra design check point formulation.

condition after thinking about the different response data. The characterization of ITZ loaded NLCs (F1-F10) and the results of the lack of fit test statistical analysis and model summary for mean particle size, EE, and drug release are summarized in Tables 2 and 3.

3.2. Particle size

The mean particle size (Y1) of prepared formulations (F1-F10) varied from 150.67 nm to 179.12 nm (Table 2). A quadratic equation was formulated to express the effect of independent variables on mean particle size, which is as follows:

$$\text{Particle size } (Y1) = 156.67 - -19.33\ X_1 - 18.50\ X_2 + 15.75\ X_1X_2$$

3.3. Entrapment efficiency

In the instance of EE, the result ranged from 60.67 ± 0.67% (F3) to 95.34 ± 1.23% (F1) depending on the variable level selected, with an average of 78 percent (Table 2). The equation below demonstrated the influence of several independent variables on EE:

$$\text{EE } (Y_2) = 8.89 + 50X_1 + 5.83X_2 - .825X_1X_2$$

3.4. In vitro ITZ release (%)

The percentage released ranged from 42.18 percent (F2) to 84.98 percent (F1), with an average of 78 percent (Fig. 2). The equation below demonstrated the influence of several independent variables on medication release:

$$Y_3 = 53.50 - -0.03083X_1 + 8.30X_2$$

3.5. Response-surface analysis and selection of formulation with optimum features

Fig. 3 represents the three-dimensional response surface plots of optimization of ITZ-loaded NLCs. When the level of polymer ratio (X_1) was increased, the particle size also increased. Effect of emulsifier (X_2) also showed positive effect (Fig. 3a). Fig. 3a demonstrated a decrease in percent cumulative release when the level of polymer ratio and emulsifier was increased simultaneously. Fig. 3c illustrates the increase in percentage EE along with an increase in polymer concentration ratio and a decrease in the concentration of emulsifiers. Based on the particle size, percentage of EE, and percentage of drug release, the optimized formulation was selected. The formulation (F6) possessed a particle size of 150.67 nm, EE of 94.65 ± 0.98 %, and drug release 68.67%, respectively.

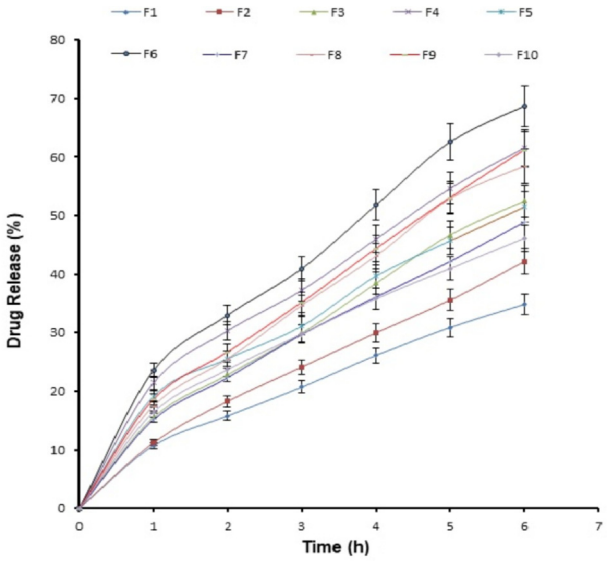

Fig. 2. *In vitro* release profile from different ITZ loaded nanostructured lipid carriers (F1-F10) performed by dialysis method using simulated saliva as dissolution medium.

3.6. DSC

Fig. 4 illustrates the results of the DSC thermograms of ITZ, poloxamer, blank NLCs, and ITZ-NLCs (F6). The melting endothermic peaks of ITZ and poloxamer were found to be 167.9 °C and 69.3 °C, respectively. The melting point of blank NLCs, on the other hand, was lowered to 65.0 °C.

3.7. TEM

TEM examination of formulation F6 showed the spherical-shaped particles with low size distribution as shown in Fig. 5. TEM images show that particle size is less than 180 nm that is suitable for ocular delivery.

3.8. Zeta potential

In the current study, the zeta potential value of the optimized formulation (F6) was −28 mV.

Table 3
Results of the lack of fit test statistical analysis and model summary for mean particle size, entrapment efficiency, and drug release.

Dependent variables			Y_1 = Particle size				Y_2 = Entrapment efficiency					Y_3 = Drug release					
Source of variation	DF	SS	MS	F	P	DF	SS	MS	F	P	DF	SS	MS	F	P	DF
Model	5	6467.85	1293.57	38.20	0.0018[a]	5	1225.49	245.10	2.50	0.0015[a]	5	764.82	152.96	0.9484	0.0014[a]	764.82
A-Lipid Ratio	1	5164.43	5164.43	152.51	0.0002	1	729.74	729.74	7.44	0.0526	1	115.98	115.98	0.7191	0.4442	115.98
B-Emulsifier	1	0.6734	0.6734	0.0199	0.8947	1	9.91	9.91	0.1010	0.7665	1	144.65	144.65	0.8969	0.3972	144.65
AB	1	48.16	48.16	1.42	0.2989	1	1.45	1.45	0.0148	0.9090	1	479.61	479.61	2.97	0.1597	479.61
A^2	1	1254.58	1254.58	37.05	0.0037	1	185.65	185.65	1.89	0.2409	1	16.35	16.35	0.1014	0.7661	16.35
B^2	1	34.27	34.27	1.01	0.3714	1	218.19	218.19	2.22	0.2101	1	12.27	12.27	0.0761	0.7964	12.27

DF; degree of freedom, SS; sum of squares, MS; mean of square, F; F-value, P; P-value. [a]Statistically significant ($p < 0.05$).

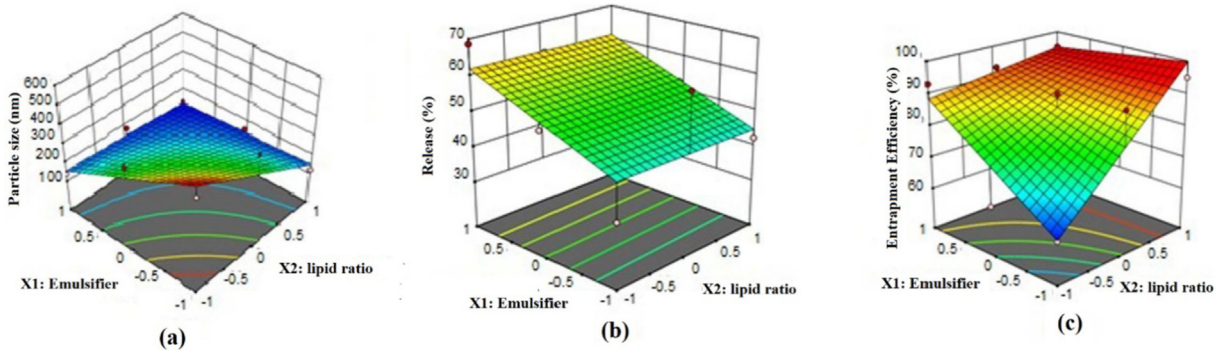

Fig. 3. Response surface plot showing the effect of lipid ratio (X_1) and % emulsifier (X_2) on particle size, entrapment efficiency, and release.

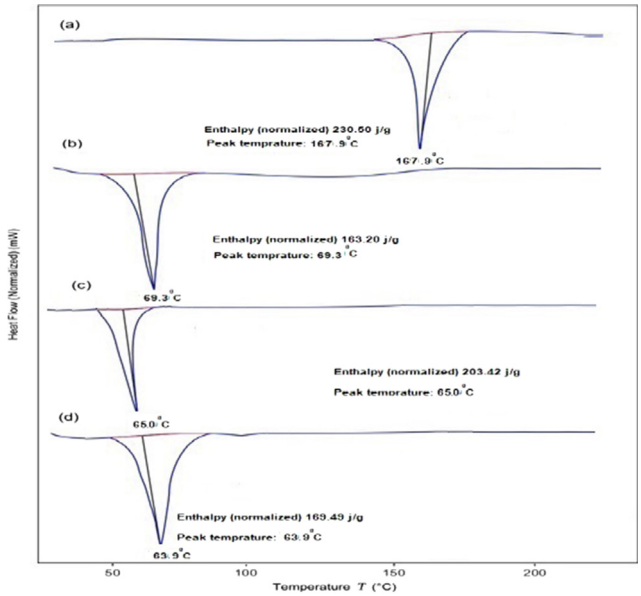

Fig. 4. DSC of (a) Itraconazole, (b) Poloxamer, (c) Blank NLCs; (D) ITZ-NLCs (F6).

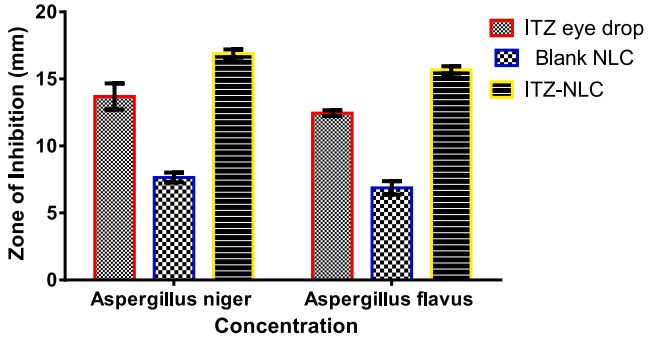

Fig. 6. Zone of inhibition of optimized itraconazole-loaded nanostructured lipid carrier (ITZ-NLC, F6), blank NLC, and ITZ eye drop (standard).

3.9. Antifungal activity

Zone of inhibition of optimized ITZ-loaded nanostructured lipid carrier (ITZ-NLC, F6), blank NLC, and ITZ eye drop (standard) are presented in Fig. 6. The zone of inhibition contributed by F6 was estimated to be 16.89 ± 0.31 mm and 15.67 ± 0.28 mm against *Aspergillus niger* and *Aspergillus flavus* respectively, which was higher than the zone of inhibition produced by commercial solution i.e., ITZ eye drop (13.69 ± 0.98 mm and 12.45 ± 0.21 mm against *Aspergillus niger* and *Aspergillus flavus,* respectively).

3.10. Irritation potential

The irritation potential of the F6 was tested using the HET-CAM method. Positive control (0.1 M sodium hydroxide) and negative control (0.9% sodium chloride) (practically non-irritant) were used for comparison and the test was performed as described earlier (Neupane et al., 2014). The results of the test are shown in Table 4 and Fig. 7.

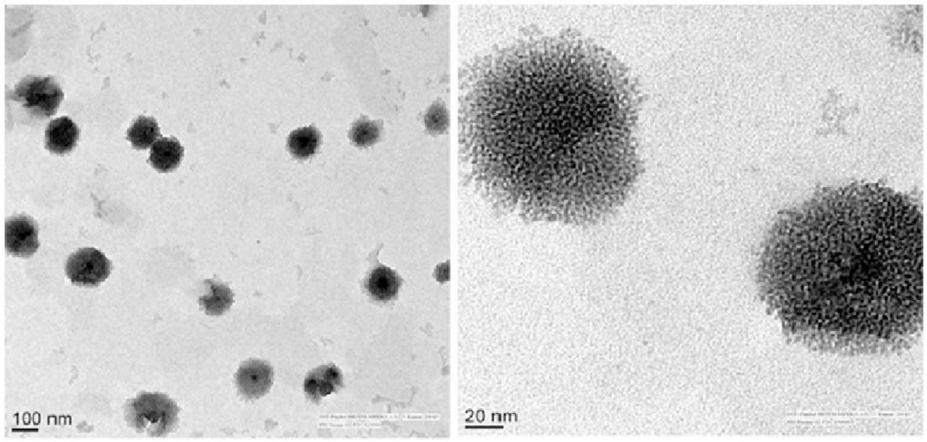

Fig. 5. Transmission electron microscopy image of optimized itraconazole loaded nanostructured lipid carrier (F6).

Table 4
Scores obtained in the ocular irritancy study by the HET-CAM test.

Samples tested	Irritation scores (time in min)				
	5	60	240	480	720
ITZ-loaded NLCs (F6)	0	0	0	0	0.36
Negative control (0.9% w/v sodium chloride)	0	0	0	0	0
Positive control (0.1 M sodium hydroxide)	3	3	3	3	3

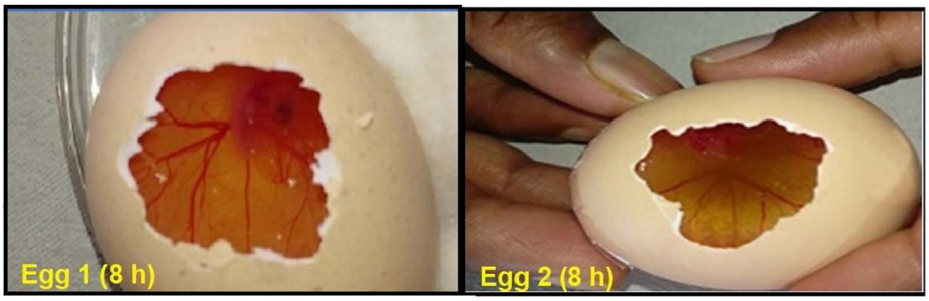

Fig. 7. Ocular tolerance test (HET-CAM) of optimized itraconazole loaded nanostructured lipid carrier (F6) at 8 h.

4. Discussion

The human eye is directly exposed to the environment which makes it more sensitive to several fungal infections. Human eyes have inherent protective mechanisms such as continuous tear flow, presence of enzymes in tear fluid besides tough corneal epithelium. However, these defense systems are ineffective once the pathogens cross the anatomical barriers, which may increase the chances of losing eyesight. Identification of the fungal eye infection at the right time and treatment with an effective antifungal agent increases chances of early cure without loss of vision. Several infections like filamentous fungal infections caused by *Fusarium-solani* and *Aspergillus flavus*, fungal endophthalmitis and chorioretinitis, and infections due to Candida spp., Curvulariaspp, and Acanthamoebae spp. are the most commonly observed ophthalmic fungal infections (Klotz et al., 2000). People using contact lens and patients with AIDS are also vulnerable to fungal eye infections (Butrus and Klotz, 1986; Hemady, 1995).

To achieve higher concentrations of drug locally in the eye, and to minimize the systemic adverse events, we designed an ocular delivery system. The clinical efficacy of an antifungal agent for ocular therapy of fungal infection depends mainly on the concentration achieved in the corneal tissue. Therefore, amphotericin B although was a choice of drug is now replaced due to its toxicity and other limitations. A triazole derivative, ITZ is highly effective against aspergillosis, however, has poor water solubility (Pardeike et al., 2016). After oral administration, ITZ exhibits poor bioavailability, and also its systemic use is limited due to hepatotoxicity. Being lipophilic, ITZ can cross the lipid-rich corneal epithelium and endothelium, however, exhibits limited penetration through the corneal stroma. The use of a nanoparticulate system can effectively improve its corneal penetration (Kalavathy et al., 2005).

NLC offers an effective nanoparticulate carrier system for poorly water-soluble drugs, which is made of a blend of a solid lipid and a liquid lipid (oil). Apart from increasing the solubility and permeability, NLC offers extremely low toxicological potential as they are made from GRAS-certified digestible excipients. Literature signifies that the natural polymers, isolated from plant seeds by simple process (Anroop et al., 2005) have also been used in preparing lipid-based nanoparticles (Mai et al., 2020). The composition used in the current study including stearic acid, oleic acid, and poloxamer is widely used in ocular therapy (Nair et al., 2021b). A three-level factorial plan was utilized for developing the NLC of ITZ and to study the impact of polymer and surfactant on different parameters like % EE, particle size, and drug release to choose the best (enhanced) definition. ANOVA was applied to determine the significance and magnitude of the interaction between independent and dependent variables (Shah et al., 2019a) at a 5% significance level. A model is considered significant if the p-value (significance probability value) is less than 0.05. The regression model was used to generate a 3D surface to analyze nine interactions of the independent variables.

The size of the particles plays important role in improving the rate of dissolution as well as in their adhesion and interaction with biological cells (Foster et al., 2001). As illustrated by the negative value preceding the variable in quadratic equation no. 4, the variables X_1, X_2 had a negative impact on particle size, Y_1. A higher emulsifier-to-lipid ratio encourages the creation of smaller particles and boosts the stability of the nanosystem by reducing the interfacial tension between the lipid matrix and the hydrophilic phase as described in the literature (Okonogi and Riangjanapatee, 2015).

NLCs have unordered lipid crystals that can incorporate more drugs and improve the encapsulation capacity. EE indicates the effectiveness of the incorporated drug into the carrier system. The higher the solubility of the drug in the mixture of lipids used allows maximum drug loading in the NLCs (How et al., 2013). It is evident from equation no. 5 that the variables X_1 and X_2 had a direct positive influence on the EE as shown by the positive sign of coefficients before the variable. Increased emulsifier-to-lipid ratios might increase EE; this could be due to the presence of a sufficient emulsifier that kept the ITZ within the lipid particles and/or on their surface. Thus, the ratio of liquid to lipids has a direct effect on EE, which can be attributed to the increased availability of liquid lipid for chemical entrapment. Imperfect crystal formation in the lipid nanoparticle is usually achieved when solid lipid is mixed with liquid lipid, which provided added advantage of higher drug loading of NLC (Müller et al., 2002). The reason behind higher drug loading is mainly due to highly unordered lipid structures formed in NLC. Thus, the drug can be present in between the fatty acids, lipid layers, or in imperfections found in crystallized structures of solid-lipid.

It is highly essential to have a drug delivery system that possesses a better drug release capacity which will assure improved effectiveness and reduced side effects of the drug. The beneficial influence of factors X_1 and X_2 on drug release may be observed in equation no. 6 as the positive value preceding these variables. The release study demonstrated biphasic drug release behavior with an initial burst release phase up to 2 h followed by a sustained drug release phase until 6 h (Fig. 2). The higher amount of drug release in the initial period could be related to the drug molecules present on the surface of the carriers. In addition, the higher emulsifier-to-lipid ratio could also have played a bigger role in enhancing the ITZ release. The literature describes that the various factors that could influence the drug release from NLCs, including the interactions that occur between the drug and excipients, desorption of the surface-bound/adsorbed drug, drug diffusion through nanoparticles lipid matrix, degradation/erosion of the matrix materials, and drug solubility in the lipid (Nair et al., 2021a). On the other hand, the permeation of molecules across the biological membrane is generally influenced by the physicochemical properties of the permeant as well as the physiological features of the membrane (Anroop et al., 2009). Nevertheless, the release rate is dependent on the particle size of the NLCs. Smaller size represents the huge surface area available for solvation and diffusion of solubilized drugs in the surrounding environment. Higher particle size would result in slower drug release due to reduced surface area. Further, physical modification such as reducing the particle size and altering the crystal habit is the frequently utilized technique to enhance the drug solubility of poorly aqueous soluble drugs (Khadka et al., 2014). Particle size is dependent on the polymer or drug ratio. The rapid release can also be attributed to the amorphous nature of ITZ inside NLCs. It is worthwhile to mention here that several complex colloidal structures such as supercooled melts, mixed micelle, micelle, liposomes exist simultaneously along with lipid nanoparticles in NLC. Though difficult to evaluate, the drug distribution between these coexisting colloidal species is significant since the dynamic phenomenon can influence drug release kinetics and dissolution (Mehnert and Mäder, 2001).

The DSC is a thermal technique used to inspect the crystalline properties and to screen for any possible interactions between the drug and the excipients in ITZ-NLC. The variation in the melting point observed with Poloxamer (69.3 °C to 65.0 °C) could be due to the presence of surfactant (Lv et al., 2009; Solanki et al., 2018). Because of the incorporation of ITZ into the lipid matrix, the melting point of ITZ-NLCs was further reduced to 63.9 °C as a result of disordered crystal structure arrangement. In ITZ-NLCs, the sharp endothermic peak for ITZ was absent, implying that ITZ was in an amorphous state. Comparative discoveries were reported by for DSC examination of lipid-based nanoparticles (Lv et al., 2009).

The particle size of the nanoparticles indicates the average diameter of the nanoparticle. It is crucial to confirm that the size of the nanoparticle formulated is within the nano-sized range using imaging studies. TEM images of ITZ NLCs show that the particles are circular in shape, discrete, and are relatively uniform indicating good particle dispersity. There seems to be a minor difference in size analyzed in TEM and that was determined using a zeta sizer. Size analysis is greatly affected by the conditions, method of analyzing data and also depends on the operation of the instrument in the determination. Such a small difference is attributed to the differences in the techniques and method of data analysis between both instruments as zeta sizer measures the hydrodynamic size of particles and in a liquid state.

The zeta potential is shown to be critical for the colloidal stability of nanoparticles in solution and is used basically to achieve a high level of physical steadiness (Jacob et al., 2020). As a rule, a large zeta potential prevents particles from aggregating via electric repulsion. In general, zeta potential ranging from − 5 mV to +5 mV will offer low stability to the dispersed system and there are higher chances of particle aggregation (Shah et al., 2019b). Zeta potential must be higher than +30 mV or lower than −30 mV to get stability due to electric repulsion. However, when polymeric surfactants are used while making NLCs, steric stabilization is also achieved because of nonionic surfactants and having polymeric chains. Indeed, the observed value in the F6 NLC signifies the charged particles are likely to have moderate repulsion and eventually will reduce the flocculation and perhaps could stabilize the system (Morsy and Nair, 2018; Shah et al., 2021). In addition, the formulation contains a nonionic surfactant (Poloxamer 407), which has a large hydrophobic segment and a long hydrophilic polyethylene glycol chain, which generally have a negative charge and are likely to produce repulsion between the carriers (ElMeshad and Mohsen, 2016).

Aspergillosis comprises a variety of manifestations of infection affecting both humans and animals. Their growing resistance to azoles, the primary treatment in the management of human aspergillosis, is an alarming problem around the world. One of the most effective triazole drugs to treat aspergillosis presently includes ITZ available as oral and intravenous dosage form (Arastehfar et al., 2021). Chronic oral therapy of ITZ may also play a key role in ocular infections such as Aspergillus endophthalmitis and keratomycosis since the drug penetrates the deeper corneal layers (Ozdemir et al., 2012). The efficacy of the prepared formulation depends on its potential to demonstrate antifungal activity as well. Therefore, the pharmacodynamic effect of ITZ in prepared nanocarriers was evaluated by comparing the results of the zone of inhibition. It is evident from the results that the zone of inhibition contributed by F6 was found to be significantly higher than the zone of inhibition produced by the commercial formulation of ITZ eye drop. When the level of significance was tested using Understudy's *t*-test, ($p < 0.0001$) a critical distinction in the ITZ movement of reference method and F6 was observed. Thus, it was confirmed that the antifungal activity of F6 was more than the marketed formulation.

Developing an optimum ophthalmic formulation needs analysis of the irritation potential of the formulation on the ocular tissues. HET-CAM assay is a rapid and inexpensive tool to measure the irritation potential of pharmaceutical formulations. CAM has blood vessels that generate from the allantoic arteries and veins and serve as a respiratory membrane that covers the chick embryo. Changes in blood vessels after treatment would indicate conjunctival damages and toxicity of the product. Sodium hydroxide is used as a positive control that causes hyperemia, hemorrhage, and clotting on the blood vessels of the CAM surface. It is an alternative technique for animal-based methods because of its rapid and visible response to irritant substances. Additionally, there is a similarity between the CAM blood vessels and vascularized mucosal tissue of the human eyes. About ethical duties, this testing does not conflict with the fact that hatched eggs serve as a borderline case in a method that involves testing in both *in vivo* and *in vitro* systems. Within the mature HET-CAM test, the full inflammatory process produced by widespread growth of vascular stratified tissues and capillaries may be observed in the conjunctival tissue of rabbit eyes. A mean score of zero was seen during the twelve-hour trial for the negative control, which essentially shows no irritating impact, whereas a mean score of three was observed throughout the twelve-hour research for the positive control, which practically suggests a severe irritant effect. After 8 h, a barely visible membrane darkening (Fig. 7) caused by HET-CAM test exposure to F6 was observed in test eggs. Thus, with a mean score of 0 after 8 h (Table 4) F6 may be classified as less irritating. Concerning eye tissue, one possible description is that an ocular formulation remains in touch for a brief period and that even after

repeated usage for 8 h, no irritation ensured the F6′s safety (Jaiswal et al., 2015).

5. Conclusion

ITZ, an anti-fungal drug with high therapeutic efficacy against *Aspergillus* was successfully encapsulated in NLCs for ophthalmic application. The NLCs were successfully formulated by the high-speed homogenization technique. The 3^2 fractional design revealed that the formulation components (lipid ratio- X_1 and percentage of emulsifier-X_2) influence the dependent variables. Both the lipid ratio and emulsifier have a positive effect on percentage entrapment efficiency and percentage release. Indeed, the optimized formulation possesses nano size (less than 200 nm), good entrapment efficiency (∼78%), and steady drug release. Antifungal studies demonstrated that the developed NLCs possess adequate activity as compared to the commercial formulation. Finally, the results of the HET-CAM test suggest that the formulation F6 is safe and non-irritant for the ocular application, though needs to be evaluated *in vivo*. The current approach being noninvasive, it is likely to be preferred by the patients over the exiting therapy. Overall, the data here demonstrated that the optimized ITZ-loaded NLCs could be an effective approach for the treatment of ocular fungal infections that would otherwise be difficult to treat with conventional dosage forms.

Funding

Majid Alhomrani would like to acknowledge TURSP (2020/257).

Declaration of Competing Interest

The authors declare that they have no known competing financial interests or personal relationships that could have appeared to influence the work reported in this paper.

Acknowledgments

The authors are thankful to AlMaarefa University in Riyadh for providing support to do this research.

References

Achouri, D., Alhanout, K., Piccerelle, P., Andrieu, V., 2013. Recent advances in ocular drug delivery. Drug. Dev. Ind. Pharm. 39 (11), 1599–1617.

Akrawi, S.H., Gorain, B., Nair, A.B., Choudhury, H., Pandey, M., Shah, J.N., Venugopala, K.N., 2020. Development and optimization of naringenin-loaded chitosan-coated nanoemulsion for topical therapy in wound healing. Pharmaceutics 12 (9), 893. https://doi.org/10.3390/pharmaceutics12090893.

Anroop, B., Bhatnagar, S.P., Ghosh, B., Parcha, V., 2005. Studies on Ocimum gratissimum seed mucilage: evaluation of suspending properties. Indian J. Pharm. Sci. 67 (2), 206–209.

Anroop, B., Ghosh, B., Parcha, V., Khanam, J., 2009. Transdermal delivery of atenolol: effect of prodrugs and iontophoresis. Curr. Drug Deliv. 6 (3), 280–290.

Arastehfar, A., Carvalho, A., Houbraken, J., Lombardi, L., Garcia-Rubio, R., Jenks, J.D., Rivero-Menendez, O., Aljohani, R., Jacobsen, I.D., Berman, J., Osherov, N., Hedayati, M.T., Ilkit, M., Armstrong-James, D., Gabaldón, T., Meletiadis, J., Kostrzewa, M., Pan, W., Lass-Flörl, C., Perlin, D.S., Hoenigl, M., 2021. Aspergillus fumigatus and aspergillosis: from basics to clinics. Stud. Mycol. 100, 100115. https://doi.org/10.1016/j.simyco.2021.100115.

Balguri, S.P., Adelli, G.R., Majumdar, S., 2016. Topical ophthalmic lipid nanoparticle formulations (SLN, NLC) of indomethacin for delivery to the posterior segment ocular tissues. Eur. J. Pharm. Biopharm. 109, 224–235.

Butrus, S.I., Klotz, S.A., 1986. Blocking Candida adherence to contact lenses. Curr. Eye Res. 5 (10), 745–750.

Chaudhary, S., Nair, A.B., Shah, J., Gorain, B., Jacob, S., Shah, H., Patel, V., 2021. Enhanced solubility and bioavailability of dolutegravir by solid dispersion method. In vitro and *in vivo* evaluation—a potential approach for HIV therapy. AAPS PharmSciTech 22 (3), 127.

Dhiman, N., Awasthi, R., Sharma, B., Kharkwal, H., Kulkarni, G.T., 2021. Lipid nanoparticles as carriers for bioactive delivery. Front Chem 9, 580118.

Duong, V.-A., Nguyen, T.-T.-L., Maeng, H.-J., 2020. Preparation of solid lipid nanoparticles and nanostructured lipid carriers for drug delivery and the effects of preparation parameters of solvent injection method. Molecules 25 (20), 4781. https://doi.org/10.3390/molecules25204781.

ElMeshad, A.N., Mohsen, A.M., 2016. Enhanced corneal permeation and antimycotic activity of itraconazole against Candida albicans via a novel nanosystem vesicle. Drug Deliv. 23 (7), 2115–2123.

Fang, C.-L., A. Al-Suwayeh, S., Fang, J.-Y., 2013. Nanostructured lipid carriers (NLCs) for drug delivery and targeting. Recent Pat. Nanotechnol. 7 (1), 41–55.

Foster, K.A., Yazdanian, M., Audus, K.L., 2001. Microparticulate uptake mechanisms of in-vitro cell culture models of the respiratory epithelium. J. Pharm. Pharmacol. 53 (1), 57–66.

Haider, M., Abdin, S.M., Kamal, L., Orive, G., 2020. Nanostructured lipid carriers for delivery of chemotherapeutics: a review. Pharmaceutics 12 (3), 288. https://doi.org/10.3390/pharmaceutics12030288.

Hallan, S.S., Sguizzato, M., Esposito, E., Cortesi, R., 2021. Challenges in the physical characterization of lipid nanoparticles. Pharmaceutics 13 (4), 549. https://doi.org/10.3390/pharmaceutics13040549.

Hemady, R.K., 1995. Microbial keratitis in patients infected with the human immunodeficiency virus. Ophthalmology 102 (7), 1026–1030.

Hoffman, J.J., Burton, M.J., Leck, A., 2021. Mycotic keratitis-a global threat from the filamentous fungi. J Fungi (Basel) 7 (4), 273. https://doi.org/10.3390/jof7040273.

How, C.W., Rasedee, A., Manickam, S., Rosli, R., 2013. Tamoxifen-loaded nanostructured lipid carrier as a drug delivery system: characterization, stability assessment and cytotoxicity. Colloids Surf. B Biointerfaces 112, 393–399.

Irimia, T., Dinu-Pîrvu, C.-E., Ghica, M., Lupuleasa, D., Muntean, D.-L., Udeanu, D., Popa, L., 2018. Chitosan-based in situ gels for ocular delivery of therapeutics: a state-of-the-art review. Mar. Drugs 16 (10), 373. https://doi.org/10.3390/md16100373.

Jacob, S., Nair, A.B., Al-Dhubiab, B.E., 2017. Preparation and evaluation of niosome gel containing acyclovir for enhanced dermal deposition. J. Liposome Res. 27 (4), 283–292.

Jacob, S., Nair, A.B., Shah, J., 2020. Emerging role of nanosuspensions in drug delivery systems. Biomater. Res. 24 (1), 1–16.

Jaiswal, M., Kumar, M., Pathak, K., 2015. Zero order delivery of itraconazole via polymeric micelles incorporated in situ ocular gel for the management of fungal keratitis. Colloids Surf. B Biointerfaces 130, 23–30.

Kalavathy, C.M., Parmar, P., Kaliamurthy, J., Philip, V.R., Ramalingam, M.D., Jesudasan, C.A., Thomas, P.A., 2005. Comparison of topical itraconazole 1% with topical natamycin 5% for the treatment of filamentous fungal keratitis. Cornea 24 (4), 449–452.

Kamboj, S., Bala, S., Nair, A.B., 2010. Solid lipid nanoparticles: an effective lipid based technology for poorly water soluble drugs. Int. J. Pharm. Sci. Rev. Res. 5 (2), 78–90.

Khadka, P., Ro, J., Kim, H., Kim, I., Kim, J.T., Kim, H., Cho, J.M., Yun, G., Lee, J., 2014. Pharmaceutical particle technologies: an approach to improve drug solubility, dissolution and bioavailability. Asian J. Pharm. Sci. 9 (6), 304–316.

Klotz, S.A., Penn, C.C., Negvesky, G.J., Butrus, S.I., 2000. Fungal and parasitic infections of the eye. Clin. Microbiol. Rev. 13 (4), 662–685.

Knutsson, K.A., Iovieno, A., Matuska, S., Fontana, L., Rama, P., 2021. Topical corticosteroids and fungal keratitis: a review of the literature and case series. J. Clin. Med. 10 (6), 1178. https://doi.org/10.3390/jcm10061178.

Lim, W.M., Rajinikanth, P.S., Mallikarjun, C., Kang, Y.B., 2014. Formulation and delivery of itraconazole to the brain using a nanolipid carrier system. Int. J. Nanomed. 9, 2117–2126.

Liu, C.-H., Wu, C.-T., 2010. Optimization of nanostructured lipid carriers for lutein delivery. Colloids Surf., A 353 (2-3), 149–156.

Lv, Q., Yu, A., Xi, Y., Li, H., Song, Z., Cui, J., Cao, F., Zhai, G., 2009. Development and evaluation of penciclovir-loaded solid lipid nanoparticles for topical delivery. Int. J. Pharm. 372 (1-2), 191–198.

Mai, H.D., Tran, P.H.L., Tran, T.T.D., 2020. Solid lipid particle-loaded Ocimum gratissimum seed films and polymeric films for controlled drug delivery. Drug Delivery Lett. 10 (4), 300–307.

Mehnert, W., Mäder, K., 2001. Solid lipid nanoparticles: production, characterization and applications. Adv. Drug Deliv. Rev. 47 (2–3), 165–196.

Morrison, P.WJ., Khutoryanskiy, V.V., 2014. Advances in ophthalmic drug delivery. Ther. Deliv. 5 (12), 1297–1315.

Morsy, M.A., Nair, A.B., 2018. Prevention of rat liver fibrosis by selective targeting of hepatic stellate cells using hesperidin carriers. Int. J. Pharm. 552 (1-2), 241–250.

Morsy, M.A., Abdel-Latif, R.G., Nair, A.B., Venugopala, K.N., Ahmed, A.F., Elsewedy, H. S., Shehata, T.M., 2019. Preparation and evaluation of atorvastatin-loaded nanoemulgel on wound-healing efficacy. Pharmaceutics 11 (11).

Müller, R.H., Radtke, M., Wissing, S.A., 2002. Nanostructured lipid matrices for improved microencapsulation of drugs. Int. J. Pharm. 242 (1-2), 121–128.

Nair, A.B., Al-Dhubiab, B.E., Shah, J., Attimarad, M., Harsha, S., 2017. Poly (lactic acid-co-glycolic acid) nanospheres improved the oral delivery of candesartan cilexetil. Indian J. Pharm. Educ. Res 51 (4), 571–579.

Nair, A., Shah, J., Al-Dhubiab, B., Jacob, S., Patel, S., Venugopala, K., Morsy, M., Gupta, S., Attimarad, M., Sreeharsha, N., Shinu, P., 2021a. Clarithromycin solid lipid nanoparticles for topical ocular therapy: optimization, evaluation and in vivo studies. Pharmaceutics 13 (4), 523. https://doi.org/10.3390/pharmaceutics13040523.

Nair, A.B., Sreeharsha, N., Al-Dhubiab, B.E., Hiremath, J.G., Shinu, P., Attimarad, M., Venugopala, K.N., Mutahar, M., 2019. HPMC- and PLGA-based nanoparticles for

the mucoadhesive delivery of sitagliptin: optimization and *In vivo* evaluation in rats. Materials (Basel) 12 (24), 4239. https://doi.org/10.3390/ma12244239.

Nair, A.B., Shah, J., Jacob, S., Al-Dhubiab, B.E., Sreeharsha, N., Morsy, M.A., Gupta, S., Attimarad, M., Shinu, P., Venugopala, K.N., Sailor, G., 2021b. Experimental design, formulation and *in vivo* evaluation of a novel topical in situ gel system to treat ocular infections. PLoS ONE 16 (3), e0248857. https://doi.org/10.1371/journal.pone.0248857.

Neupane, Y.R., Srivastava, M., Ahmad, N., Kumar, N., Bhatnagar, A., Kohli, K., 2014. ipid based nanocarrier system for the potential oral delivery of decitabine: formulation design, characterization, ex vivo, and *in vivo* assessment. Int. J. Pharm. 477 (1–2), 601–612.

Okonogi, S., Riangjanapatee, P., 2015. Physicochemical characterization of lycopene-loaded nanostructured lipid carrier formulations for topical administration. Int. J. Pharm. 478 (2), 726–735.

Ozdemir, H.G., Oz, Y., Ilkit, M., Kiraz, N., 2012. Antifungal susceptibility of ocular fungal pathogens recovered from around the world against itraconazole, voriconazole, amphotericin B, and caspofungin. Med. Mycol. 50 (2), 130–135.

Pandey, M., Choudhury, H., binti Abd Aziz, A., Bhattamisra, S.K., Gorain, B., Su, J.S.T., Tan, C.L., Chin, W.Y., Yip, K.Y., 2021. Potential of stimuli-responsive in situ gel system for sustained ocular drug delivery: recent progress and contemporary research. Polymers (Basel) 13 (8), 1340. https://doi.org/10.3390/polym13081340.

Pardeike, J., Weber, S., Zarfl, H.P., Pagitz, M., Zimmer, A., 2016. Itraconazole-loaded nanostructured lipid carriers (NLC) for pulmonary treatment of aspergillosis in falcons. Eur. J. Pharm. Biopharm. 108, 269–276.

Permana, A.D., Utami, R.N., Layadi, P., Himawan, A., Juniarti, N., Anjani, Q.K., Utomo, E., Mardikasari, S.A., Arjuna, A., Donnelly, R.F., 2021. Thermosensitive and mucoadhesive in situ ocular gel for effective local delivery and antifungal activity of itraconazole nanocrystal in the treatment of fungal keratitis. Int. J. Pharm. 602, 120623. https://doi.org/10.1016/j.ijpharm.2021.120623.

Shah, H., Nair, A.B., Shah, J., Bharadia, P., Al-Dhubiab, B.E., 2019a. Proniosomal gel for transdermal delivery of lornoxicam: optimization using factorial design and *in vivo* evaluation in rats. Daru 27 (1), 59–70.

Shah, J., Nair, A.B., Jacob, S., Patel, R.K., Shah, H., Shehata, T.M., Morsy, M.A., 2019b. Nanoemulsion based vehicle for effective ocular delivery of moxifloxacin using experimental design and pharmacokinetic study in rabbits. Pharmaceutics 11 (5), 230. https://doi.org/10.3390/pharmaceutics11050230.

Shah, J., Nair, A.B., Shah, H., Jacob, S., Shehata, T.M., Morsy, M.A., 2020. Enhancement in antinociceptive and anti-inflammatory effects of tramadol by transdermal proniosome gel. Asian J. Pharm. Sci. 15 (6), 786–796.

Shah, H., Nair, A.B., Shah, J., Jacob, S., Bharadia, P., Haroun, M., 2021. Proniosomal vesicles as an effective strategy to optimize naproxen transdermal delivery. J. Drug Delivery Sci. Technol. 63, 102479. https://doi.org/10.1016/j.jddst.2021.102479.

Sharif Makhmal Zadeh, B., Niro, H., Rahim, F., Esfahani, G., 2018. Ocular delivery system for propranolol hydrochloride based on nanostructured lipid carrier. Sci. Pharm. 86 (2), 16. https://doi.org/10.3390/scipharm86020016.

Solanki, N., Gupta, S.S., Serajuddin, A.T.M., 2018. Rheological analysis of itraconazole-polymer mixtures to determine optimal melt extrusion temperature for development of amorphous solid dispersion. Eur. J. Pharm. Sci. 111, 482–491.

Song, A., Deshmukh, R., Lin, H., Ang, M., Mehta, J.S., Chodosh, J., Said, D.G., Dua, H.S., Ting, D.S.J., 2021. Post-keratoplasty infectious keratitis: epidemiology, risk factors, management, and outcomes. Front Med (Lausanne) 8, 707242.

Sreeharsha, N., Rajpoot, K., Tekade, M., Kalyane, D., Nair, A.B., Venugopala, K.N., Tekade, R.K., 2020. Development of metronidazole loaded chitosan nanoparticles using QbD approach-a novel and potential antibacterial formulation. Pharmaceutics 12 (10), 920. https://doi.org/10.3390/pharmaceutics12100920.

Thomas, P.A., 2003. Fungal infections of the cornea. Eye (Lond) 17 (8), 852–862.

Wissing, S.A., Müller, R.H., 2001. A novel sunscreen system based on tocopherol acetate incorporated into solid lipid nanoparticles. Int. J. Cosmet Sci. 23 (4), 233–243.